# Analytical description of the sputtering yields of silicon bombarded with normally incident ions

Klaus Wittmaack
*GSF-National Research Center for Environment and Health, Institute of Radiation Protection, 85758 Neuherberg, Germany*
(Received 17 January 2003; revised manuscript received 17 April 2003; published 29 December 2003; publisher error corrected 14 January 2004)

Experimentally determined sputtering yields of silicon bombarded with normally incident ions were analyzed with the aim of deriving a complete analytical description of the data. The yields, covering a wide range of energies (from 50 eV to 540 keV) and primary ions of vastly different mass (from H to Xe), can be described in universal form using (i) two energy-dependent functions, the reduced nuclear stopping cross section $s_n$ and Bohdansky's threshold function $\eta$, (ii) a modified form of Sigmund's $\alpha$ function, only dependent on the mass ratio of projectile and target atoms, and (iii) a constant calibration factor $\tilde{x}_0 N/\tilde{E}_s$, where $\tilde{x}_0$ is the effective mean escape depth of sputtered atoms, $N$ the number density of Si atoms, and $\tilde{E}_s$ an effective surface binding energy. Considering the fact that according to computer simulations the mean escape depth increases significantly with increasing projectile energy, the observed constancy of $\tilde{x}_0 N/\tilde{E}_s$ requires the assumption that $\tilde{E}_s$ is not a constant but contains two terms, the ''true'' surface binding energy $E_s$ and an additional energy-dependent term presumably reflecting the fraction of deposited energy that is lost in inelastic processes as well as in creating phonons and damage. There are indications that the sputtering yields reported for H and D bombardment as well as for heavy-ion impact at very low energies are too small by factors up to about 2, presumably due to oxygen incorporation and/or growth of surface contamination layers under nonideal vacuum conditions.

DOI: 10.1103/PhysRevB.68.235211 PACS number(s): 79.20.Rf

## I. INTRODUCTION

The analytical theory of sputtering due to nuclear interactions (knock-on sputtering) was developed by Sigmund.[1] According to theory the sputtering yield $Y$ for normally incident ions (or atoms) of mass $M_1$, atomic number $Z_1$, and energy $E$ can be factorized in the form

$$Y = Y(E,\mu,Z_1,Z_2) = (x_0 N/\pi^2 E_s)\alpha S_n, \tag{1}$$

where $x_0$ is the mean depth of origin of sputtered atoms, $N$ the number density of target atoms $(M_2,Z_2)$, and $\mu = M_2/M_1$. Here $E_s$ is the surface potential barrier (surface binding energy), $S_n = -N^{-1}(dE/dx)_n$ the nuclear stopping cross section, and $\alpha = \alpha(\mu,E)$ a dimensionless function which defines the amount of energy, relative to $(dE/dx)_n$, which is deposited near the surface into nuclear motion ($x$ is the initial direction of ion beam propagation). $S_n = S_n(E,\mu,Z_1,Z_2)$ may be expressed in terms of a reduced (universal) cross section $s_n = s_n(\varepsilon)$. With $S_n$ in units of eV/atoms cm$^{-2}$,

$$S_n = 22.2\{Z_1 Z_2/Z_{12}^*(1+\mu)\}a_0^2 E_R s_n. \tag{2}$$

$E_R$ (13.6 eV) is the Rydberg energy and $a_0$ ($0.529 \times 10^{-8}$ cm) the Bohr radius. $Z_{12}^*$ is the scaling parameter for the screening radius $a_i$ of interatomic potentials, $a_i = 0.885 a_0/Z_{12}^*$. Bohr[2] suggested

$$Z_{12}^* \equiv Z_B^* = (Z_1^{2/3} + Z_2^{2/3})^{1/2}. \tag{3a}$$

In search of a universal interatomic potential, Ziegler *et al.*[3] found the best scaling of calculated screening functions using the scaling parameter

$$Z_{12}^* \equiv Z_{\mathrm{ZBL}}^* = Z_1^{0.23} + Z_2^{0.23} \tag{3b}$$

According to Lindhard *et al.*,[4] the ion energy $E$ may be converted to the reduced energy $\varepsilon$ as

$$\varepsilon = \{0.443/(1+\mu^{-1})Z_1 Z_2 Z_{12}^*\}E/E_R. \tag{4}$$

Combining Eqs. (1) and (2), the sputtering yield takes the form

$$Y = k_n \alpha s_n, \tag{5}$$

with

$$k_n = 0.858(x_0 N/E_s)Z_1 Z_2/Z_{12}^*(1+\mu), \tag{6}$$

the areal density $x_0 N$ being counted in units of $10^{15}$ atoms/cm$^2$, the surface binding energy $E_s$ in eV.

In his pioneering work, Sigmund[1] calculated $x_0$ on the basis of a low-energy interaction potential derived by extrapolation from higher energies. The resulting number turned out to be rather large, $x_0 N = 4.15 \times 10^{15}$ atoms/cm$^2$, equivalent to about three atomic layers. To get reasonable agreement between experimental and theoretical sputtering yields, the surface binding energy for silicon had to be set equal to the comparatively large cohesive energy (7.83 eV).[1] Hence the ratio $x_0 N/E_s$ should be about $5 \times 10^{14}$ atoms cm$^{-2}$ eV$^{-1}$. If the sublimation energy of Si (4.7 eV) had been used instead of the cohesive energy, the agreement would have been rather poor. The problem was partly solved by refined calculations[5] which showed that the extrapolated potential originally used by Sigmund[1] was significantly too low. The improved calculation reduced $x_0 N$ to about half the original value so that the appropriate value of $x_0 N/E_s$ could be obtained on the basis of the common assumption that $E_s$ equals the sublimation energy of the target material. Recent experiments[6] and computer simulations,[7,8] however, showed that the escape depth for ion impact at a few keV is actually

 

a factor of 4 lower than the original estimate, i.e., $x_0N = (1.0 \pm 0.2) \times 10^{15}$ atoms/cm$^2$ or $0.74 \pm 0.15$ of the mean atomic distance $1/N^{1/3} = 0.272$ nm. Using this result, $x_0N/E_s$ would turn out to be too small by a factor of about 2. The computer simulations[7,8] also showed that the depth of origin increases with increasing ejection energy of sputtered atoms and, last but not least, depends significantly on the bombardment parameters.[8] These results raise the question whether the calibration factor $x_0N/E_s$ in the analytical theory can really be considered a constant or whether this parameter is energy dependent.

Irrespective of the problems associated with an absolute calibration of the analytical yield formula, the sputtering yields observed at low impact energies are much lower than predicted by Eq. (5) because the energy and momentum distributions of recoil atoms are truncated at their high end, more so the lower the energy $E$. To account for these ''threshold effects,'' Bohdansky[9] replaced Eq. (5) by

$$Y = k_n \alpha s_n \eta. \tag{7}$$

The threshold function $\eta$ in Eq. (7) depends only on $E$ and the threshold energy $E_{\rm th}$,

$$\eta = \{1 - (E_{\rm th}/E)^{2/3}\}(1 - E_{\rm th}/E)^2. \tag{8}$$

An important aspect of Eq. (8) is that threshold effects determine the sputtering yield not only at very low energies but up to $E/E_{\rm th}$ ratios exceeding 100. For example, $\eta$ amounts to 0.5, 0.9, and 0.95 for $E/E_{\rm th} = 6.3$, 58, and 145, respectively.

For light-ion bombardment, the minimum energy required for sputtering, $E_{\rm min} = E_{\rm th}$, can be estimated from the kinematics of an event involving 180° scattering of the incident ion in the second layer of the sample, followed by a head-on collision of the reflected ion with a surface atom. Then[10]

$$E_s = \gamma(1 - \gamma)E_{\rm th}, \tag{9}$$

with

$$\gamma = 4M_1M_2/(M_1 + M_2)^2. \tag{10}$$

Equation (7) may be rearranged to define a reduced sputtering yield $y_n$ as

$$y_n = Y/k_n\alpha = s_n\eta. \tag{11}$$

At sufficiently high values of the ratio $E/E_{\rm th}$, Eq. (11) simplifies to the previously used relation[11]

$$y_n(\eta \rightarrow 1) = s_n, \tag{11a}$$

and $\alpha$ can be determined as

$$\alpha = Y(\eta \rightarrow 1)/k_n s_n, \tag{11b}$$

provided $k_n$ is known.

The purpose of this study was to explore the question whether Eq. (7) is capable of describing measured sputtering yields for a wide range of primary ion masses and energies. The starting point for this exercise was the idea that, once the appropriate energy-dependent functions $s_n$ and $\eta$ had been selected, they should be applicable to all projectile-target combinations. Hence the data evaluation was expected to provide answers to the following specific questions. (i) Can the parameter $k_n$ be considered a constant calibration factor applicable at all energies? (ii) Is $\alpha$ a function that depends only on the mass ratio $\mu$ or is it necessary to involve an energy dependence? (iii) How do the input parameters entering into the analytical model compare with the material parameters used in computer simulations? These questions are addressed on the basis of a rather broad set of experimental sputtering yield data for silicon, a material that has the advantage of being rendered amorphous by ion bombardment. Hence the effects of sample (poly)crystallinity on the sputtering yield[12] are absent.

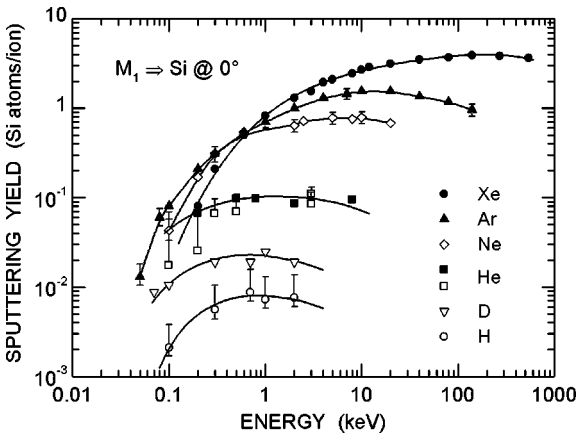


FIG. 1. Compilation of experimentally determined sputtering yields of silicon bombarded with normally incident ions. The data were derived from Refs. 11 and 13–19. The lines are drawn to guide the eye. Some error bars are included to indicate the estimated uncertainty.

## II. DATA BASIS

Experimentally determined sputtering yields of silicon are compiled in Fig. 1. Some errors bars are included which represent the estimated uncertainty of the data. The heavy-ion data were derived from a previous compilation for primary ions of Ar and Xe,[11] to which more data for 2–20 keV Ne, Ar, and Xe (Refs. 13 and 14) and low-energy results for Ar (Ref. 15) were added. Some of the heavy-ion data in Fig. 1 constitute the average of data from different groups, measured at the same or very similar energies. The measurements at energies below about 1 keV suffered from a number of uncertainties and experimental difficulties, both known and unknown. These problems cause the reported yields to differ sometimes by 30%–40%, occasionally by a factor of up to 2. In the early work of Wehner and co-workers,[16,17] for example, the (apparent) target current was enhanced by ion-induced electron emission. For neon bombardment the yields corrected for potential emission were estimated to be 25% higher than the raw data.[16] The low-energy yields measured by Zalm[13] using retarded beams, decelerated from 10–20 keV to between 2.5 keV and as low as 200 eV, were found to be systematically larger than data from other groups, the deviation increasing with decreasing impact energy. The reason is not clear. It is worth noting that the yields reported in Ref. 13 were derived from measurements of the depth of large

(~10 mm diameter) craters produced by ion beams featuring nonuniform current density distributions. The raw data were used to calculate the volume of the sputtered crater by integration. One might wonder whether the problems due to hollow beam formation, observed with decelerated beams, were larger than expected by the author.[13] It is also unclear how normal ion impact could be maintained upon retardation even though the decelerated beams were focused from 15 to 6 mm (at 200 eV) at the ''very end of their trajectory''—i.e., over a short distance. Given these uncertainties only those data of Ref. 13 that relate to nonretarded beams were included in this data compilation.

The light-ion data in Fig. 1 were also measured using decelerated beams, but at less extreme ratios of the initial-to-final energy.[18,19] Moreover, the weight-loss method was used which is insensitive to nonuniformities of the ion current density distribution at the target. The sputtering yields for proton and deuteron bombardment are quite low, equal to or less than 0.01 and 0.02 atoms/ion, respectively. Such low yields are difficult to measure because there is the danger that ion bombardment initiates the growth of surface contamination and/or the incorporation of residual gases. As a result, the rate of erosion of sample material can be reduced significantly. In extreme cases the formation of ''surface layers'' may show up in the form of a darkening of the bombarded target area.[17] The magnitude of the effect may be assessed from two sets of data reported for sputtering of Si by bombardment with He ions, represented by solid and open squares, respectively.[19] Apparently these measurements were performed at distinctly different residual gas pressures and/or different primary ion current densities. Notably at low energies the open-square yields are more than a factor of 2 lower than the solid-square yields. Eckstein *et al.* have mentioned the problem of oxide formation (see caption of Fig. 35 in Ref. 19) but did not discuss the consequences any further. In the evaluation presented below the He data represented by open squares were not taken into account.

Previously, the effect of bombardment-induced oxygen incorporation and oxide formation on sputtering yields has been studied by different groups, mostly for heavy-ion bombardment of Al (Ref. 20) and Si (Refs. 21–23) at deliberately enhanced partial pressures of oxygen. The efficiency of heavy-ion-bombardment-induced incorporation can be remarkably high, up to three oxygen atoms per 20 keV $Xe^+$ ion incident on Si.[22] A decrease in sputtering yield due to oxygen uptake may already be observed if the arrival rate of the gas molecules amounts to only 1% of the removal rate of target atoms.[20] The results of a comparative study on Mo bombarded with He and Ar suggest that the effect of oxygen exposure on the sputtering yield becomes detectably at lower oxygen-to-projectile flux ratios the lower the sputtering yield.[24] Therefore, yield measurements involving H and D projectiles should be particularly critical, but data for 2.5 keV D on Mo were not very conclusive in this respect.[24] Studies by secondary ion mass spectrometry (SIMS), on the other hand, provided evidence for oxygen incorporation in Si (Ref. 25) bombarded with 1 keV D under conditions similar to those used to measure the deuteron yields in Fig. 1. Hence it cannot be excluded that the yields for D bombardment are lower than the ''clean'' values that one would measure in the absence of oxygen incorporation. If the presumed yield reduction for D bombardment could be substantiated, one would expect the H data to be reduced even more (because the effect becomes more important the lower the sputtering yield; the error bars in Fig. 1 reflect the estimated uncertainty). For completeness we note that D-bombarded samples also showed very pronounced volume expansion and blister formation[25] at primary ion fluences between about $10^{17}$ and $10^{19}$ $cm^{-2}$, compared to typically $10^{20}$ $cm^{-2}$ in the yield measurements (fluence estimated from the quoted experimental parameters).[18,19]

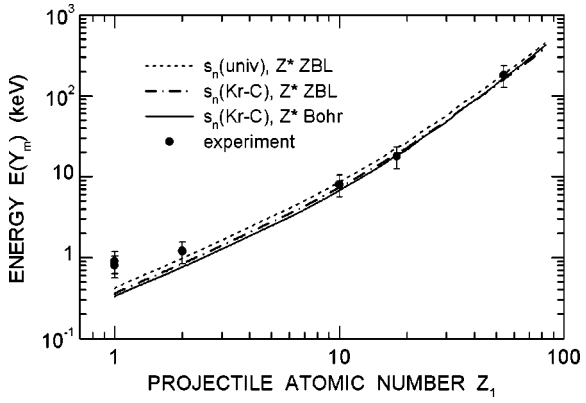


FIG. 2. Experimentally observed positions of the sputtering yield maxima (solid circles) compared with predictions derived from two different reduced nuclear stopping cross sections (dashed, dash-dotted, and solid lines).

Note that the experimental results in Fig. 1 are complete in the sense that all six sets of data include the maximum of the sputtering yield. Hence the data are very well suited for analyzing the energy dependence of the functions contained in Eq. (7).

## III. DATA EVALUATION AND DISCUSSION

### A. Reduced nuclear stopping power

In a first step of the data evaluation the measured positions $E(Y_m)$ of the sputtering yield maxima were compared with the peak positions of theoretical stopping cross section $s_n$. The experimental results are shown in Fig. 2 as solid circles. The peak positions increase monotonically with increasing $Z_1$. The experimental data for Ne, Ar, and Xe agree with the peak positions derived from two different nuclear stopping cross sections, the so-called universal cross section $s_n$(univ)[3] and the stopping cross section $s_n$(Kr-C) (Ref. 26) derived from the Kr-C potential.[27] The latter cross sections was calculated for two versions of the scaling parameter $Z_{12}^*$. The resulting difference is quite small. In view of the fact that the uncertainty in locating yield maxima in the experimental data amounts to at least $\pm 30\%$, the measured peak positions can hardly be used to make a decision in favor of one or the other theoretical stopping cross section. Hence it is necessary to inspect stopping cross sections in more detail—i.e., with respect to the absolute values and the energy dependence.

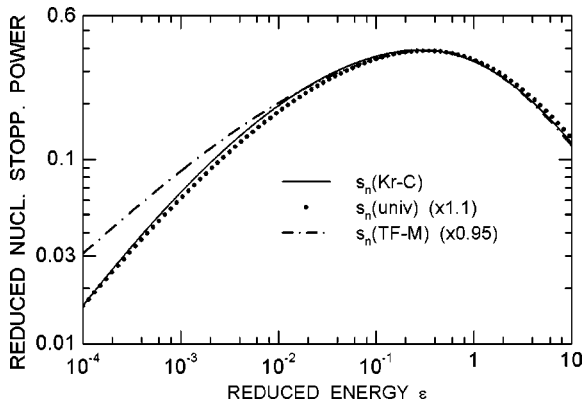


FIG. 3. Comparison of three different reduced nuclear stopping cross sections suggested in the literature. To illustrate the similarity in the region $0.01<\varepsilon<10$, two of the three cross sections were multiplied by appropriate factors.

Figure 3 shows a comparison of $s_n$(Kr-C) and $s_n$(univ) in the range of reduced energies covered by the data of Fig. 1. Also included is $s_n$(TF-$M$), the analytical fit to the Thomas-Fermi cross section after Matsunami *et al.*[28] Except for the slight differences in peak position, $s_n$(univ) is 10%–20% lower than $s_n$(Kr-C). To illustrate the close similarity in the energy dependence, $s_n$(univ) was multiplied by a factor of 1.1. Over a wide range of $\varepsilon$ values the resulting curve (dotted line in Fig. 3) is indistinguishable from $s_n$(Kr-C). In trying to fit experimental sputtering yield data to the analytical theory, the results obtained using $s_n$(univ) or $s_n$(Kr-C) will be essentially the same, except for a difference in the calibration factor $k_n$ by 10%.

A significant difference between $s_n$(Kr-C) and $s_n$(TF-M), peak adjusted by a factor 0.95, is observed at reduced energies $\varepsilon<10^{-2}$. At these energies threshold effects become dominant even for sputtering of Si by Ne, Ar, and Xe impact. To discuss the consequences, two examples of reduced sputtering yields $s_n\eta$ are presented Fig. 4, one for $s_n$(Kr-C), the other for $0.95s_n$(TF-$M$). With marginally different threshold energies (29 and 31 eV, respectively, reflecting the case Ar on Si), the reduced sputtering yields derived from the two cross sections become indistinguishable. Again we have to

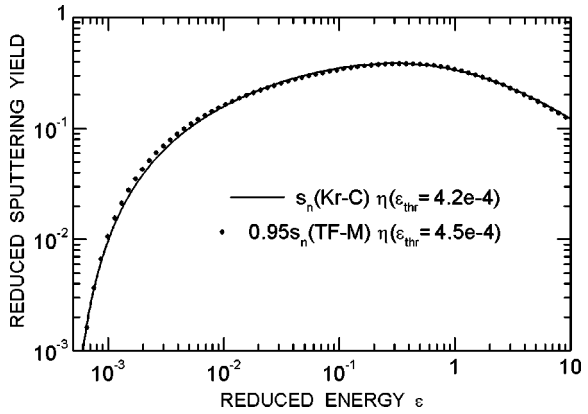


FIG. 4. Comparison of reduced sputtering yields calculated from two different stopping cross sections.

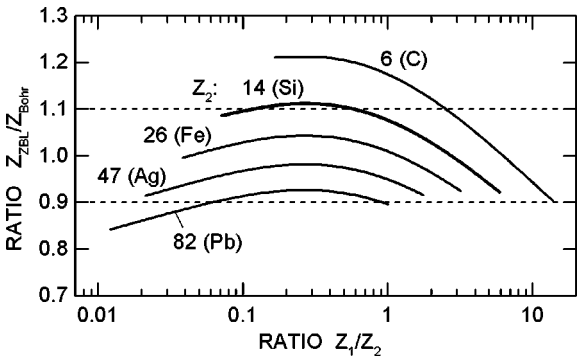


FIG. 5. Ratio of the scaling parameters $Z^*_{\mathrm{ZBL}}$ and $Z^*_{\mathrm{Bohr}}$ according to the definitions of Ziegler *et al.* and Bohr, for projectiles of atomic number $Z_1$ incident on targets with atomic number $Z_2$.

conclude that it will be difficult, if not impossible, to use sputtering yield data for identifying the most appropriate reduced nuclear stopping cross section. An additional consequence is that the derived threshold energies cannot be considered absolute numbers but will depend slightly on the choice of $s_n$. With these uncertainties in mind the somewhat arbitrary decision was made to use $s_n$(Kr-C) for further evaluations.

Another parameter that needs to be discussed is $Z^*_{12}$. As already seen from Fig. 2 the difference brought about by using the definition of either Eq. (3a) or (3b) is small. To explore the difference in more general terms, Fig. 5 shows the ratio $Z^*_{\mathrm{ZBL}}/Z^*_{\mathrm{Bohr}}$ versus $Z_1/Z_2$, calculated for five different target materials. It is evident that in most cases the difference between the two definitions of $Z^*_{12}$ is less than $\pm 10\%$ (denoted by dashed lines). Hence, in order to distinguish between $Z^*_{\mathrm{ZBL}}$ and $Z^*_{\mathrm{Bohr}}$, one needs highly accurate experimental data (e.g., for ion ranges), preferably for low- and high-mass targets. Data for medium-mass targets will only be useful if they are accurate to within about 1%. Note also that inelastic contributions to the total stopping power must be subtracted very accurately to safely determine the $Z_1$ and $Z_2$ dependence of $Z^*_{12}$. In any case, sputtering yield data are not sufficiently accurate to distinguish between the two definitions. To avoid preference in favor of either one of the definitions, the evaluation reported below was carried out using the mean of the two,

$$\overline{Z}^*_{12}=(Z^*_{\mathrm{Bohr}}+Z^*_{\mathrm{ZBL}})/2. \tag{3c}$$

The results thus obtained deviate from those using $Z^*_{\mathrm{ZBL}}$ or $Z^*_{\mathrm{Bohr}}$ by 5% or less, in either direction.

### B. Threshold function and threshold energies

Figure 6 shows the reduced sputtering yields $y_n$ derived from Fig. 1 as a function of the reduced energy $\varepsilon$. By an appropriate choice of the product $k_n\alpha$, Eq. (11), $y_n$ can be made to agree with $s_n$(Kr-C) at energies $\varepsilon>100\varepsilon_{\mathrm{th}}$ (more details of the fitting procedure are discussed with reference to Fig. 7). For the heavy-ion species Xe and Ar the agreement extends over about two orders of magnitude in energy or even more (Xe). For H and D, on the other hand, $y_n$

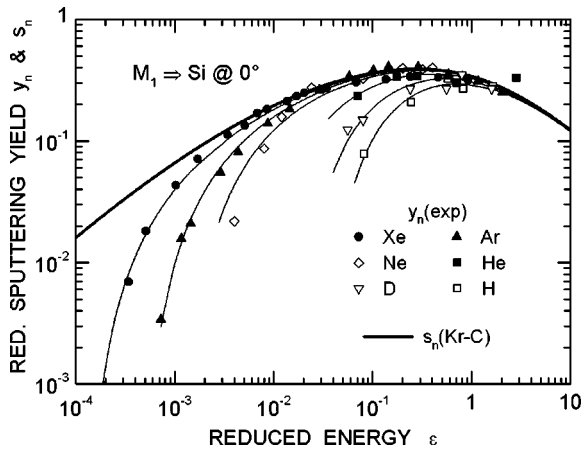


FIG. 6. Reduced sputtering yields derived from Fig. 1 vs the reduced impact energy. The reduced yields are fitted to the reduced stopping cross section $s_n$(Kr-C) (thick solid line). The thin lines represent the product of $s_n$(Kr-C) and Bohdansky's threshold function $\eta$.

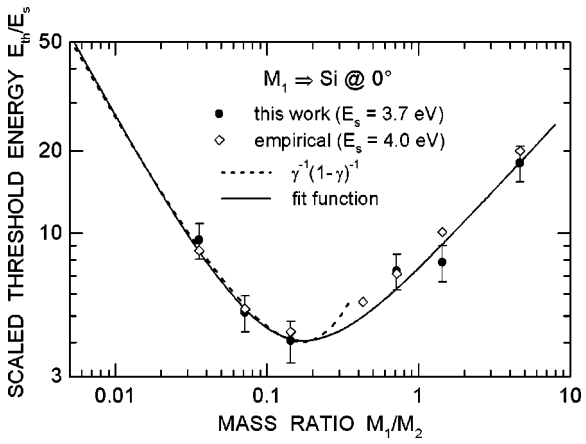


FIG. 8. Comparison of the mass dependence of scaled threshold energies $E_{\rm th}/E_s$ derived in this study (solid circles) with theoretical predictions valid for $M_2/M_1>5$ (dashed line). Also shown are empirical data from Ref. 19 (open diamonds) and a fit function covering all experimental data (solid line).

approaches $s_n$ only at the upper limit in energy covered by the experiments. With decreasing $\varepsilon$, $y_n$ tends to fall below $s_n$, more so the lower $\varepsilon$ and more readily the lower the mass of the primary ion. The deviation is due to threshold effects. The threshold effect shifts the maximum of the sputtering yield for H and D bombardment to higher energies, from $\hat{\varepsilon}=0.28$ [maximum of $s_n$(Kr-C), equivalent to 342 and 354 eV for H and D, respectively] to $\hat{\varepsilon}=0.66$ for H and to 0.56 for D (800 and 700 eV, respectively).

To determine the experimental $\eta$ values, the reduced sputtering yields $y_n$ of Fig. 6 were divided by $s_n$(Kr-C). Most of the experimental data could be fitted to within about $\pm 10\%$ to the threshold function according to Bohdansky, Eq. (8) (thin solid lines in Fig. 6). To illustrate the agreement between the experimental data and the $\eta$ functions for each projectile, ''thresholdless'' reduced sputtering yields were calculated as $y_n/\eta$. In Fig. 7 the results are compared with $s_n$(Kr-C). For each projectile the product $k_n\alpha$ was adjusted such that the mean of $y_n/\eta s_n = Y/k_n\alpha\eta s_n$, averaged over all data points per ion, was unity. With the exception of two sputtering yield data for Ne and one high-energy outlier for He, the remaining 55 individual data points for $y_n/\eta$ agree with $s_n$ to within $\pm 15\%$ or better (the low value for Ne at $\varepsilon=0.036$—i.e., 100 eV—is attributed to bombardment-induced oxygen incorporation, as discussed in Sec. II).

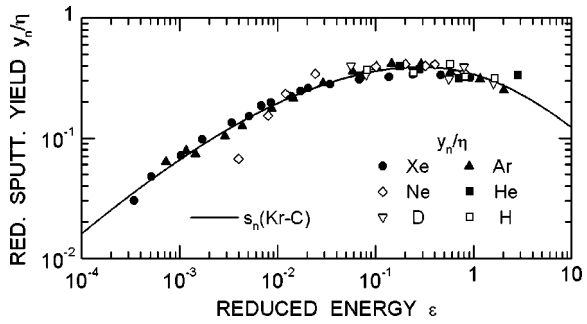


FIG. 7. Reduced sputtering yields after correction for threshold effects. The reduced nuclear stopping cross section $s_n$(Kr-C) is shown for comparison (solid line).

The results of Fig. 7 imply that the energy dependence of the sputtering yield is fully contained in the nuclear stopping cross section $s_n$ and the threshold function $\eta$. Particularly important are the results for Ar and Xe at high energies ($\varepsilon > 10^{-2}$) where threshold effects are negligible. If we assume that the calibration factor does not depend on energy (see below), the observed identity $y_n/\eta = s_n$ leads to the important conclusion that $\alpha$ is also independent of energy—i.e., only dependent on $\mu$. Inelastic contributions to stopping do not seem to have a detectable effect on $\alpha$.

For the sake of completeness we note that nonlinear (spike) effects are not expected in sputtering of light-element targets like Si bombarded with atomic ions.[29] This supposition is in accordance with the experimental data for Xe on Si which do not show any evidence for an enhancement of sputtering yields at energies between about 60 and 300 keV, corresponding to $0.1<\varepsilon<0.5$ (see Fig. 7).

The threshold energies derived from the fitting procedure are shown in Fig. 8 as $E_{\rm th}/E_s$ ratios. Theoretical $E_{\rm th}/E_s$ ratios for light-ion (H, D, and He) bombardment of Si (dashed line) were derived from Eq. (9), with $E_s=3.7$ eV. For heavy-ion impact the double-scattering concept of threshold sputtering, Eq. (9), does not apply. A good fit to the $\mu$ dependence of all experimental data can be achieved using a slightly modified version of a formula suggested by García-Rosales *et al.*,[26]

$$E_{\rm th}/E_s = a_1\mu^{-0.6} + a_2\mu, \tag{12}$$

with $a_1=7.2\pm0.2$ and $a_2=0.265\pm0.01$ (solid line in Fig. 8).

It is worth noting that the Garching group[26] has performed a similar analysis of their own sputtering yield data for a wide variety of sample materials. The analysis was based on a combination of experimental results and computer simulated data using the Monte Carlo TRIM.SP code.[30] The open diamonds in Fig. 8 represent $E_{\rm th}/E_s$ ratios derived, with $E_s$

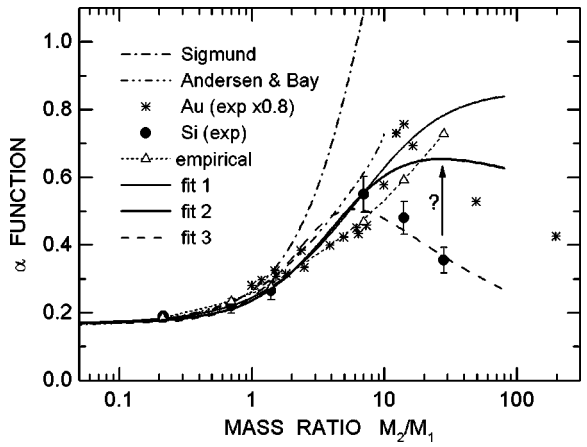


FIG. 9. Comparison of $\alpha$ values for amorphous Si, derived from the fitting procedure in Fig. 7 (solid circles), with the results of Sigmund's analytical theory (dash-dotted line, Ref. 1), an empirical fit based on experimental data of Andersen an Bay (dash–double-dotted line, Ref. 32), experimental data for polycrystalline Au (asterisks, Ref. 9), and empirical data from Ref. 19 (open triangles and dashed line). The two solid lines and the long-dashed line represent different fit functions (see text). The vertical arrow indicates the conceivable error in the $\alpha$ value for H on Si.

$=4.0$ eV, from the empirical data for $E_{\mathrm{th}}$(Si) (Ref. 19). The agreement with the present results is quite good.

### C. $\alpha$ function

To proceed further one has to make a decision concerning the absolute value of $\alpha$ for one primary ion species. Considering Sigmund's analytical sputtering theory[1] to be reliable for small mass ratios $\mu$, we set $\alpha(\mathrm{Xe\text{-}Si})=0.19$. Using Eq. (7), $\alpha$ values for the other ions (subscript $i$) were determined by way of taking ratios at $\hat{\varepsilon}$,

$$\alpha_i = \frac{(Y/k_n\eta)_{i,\hat{\epsilon}}}{(Y/k_n\eta)_{Xe,\hat{\epsilon}}}\,\alpha_{Xe}. \tag{13}$$

The results obtained this way are depicted in Fig. 9 (solid circles). Also shown is Sigmund's original estimate[1] of $\alpha$ (dash-dotted line), a refined version[31] of $\alpha$ based on experimental data of Andersen and Bay[32] (dash–double-dotted line), experimental data for polycrystalline Au (asterisks),[9] scaled by a factor of 0.8 to produce agreement with theory at mass ratios $\mu$ between 1 and 3, and empirical data (open triangles and short-dashed line),[19] scaled to $\alpha(\mathrm{Xe\text{-}Si})=0.19$. The solid lines are analytical fit functions through the experimental data, ignoring results for H and D impact,

$$\alpha=(0.168+r\mu^p)/(1+0.1\mu^q), \tag{14}$$

with $r=0.1$ (0.09), $p=1.15$ (1.4), and $q=1.18$ (1.48) for the thin (thick) solid line. If all experimental data are included, Eq. (14) may also be used to produce an analytical fit, but with $r=0.1$, $p=1.8$, and $q=2.1$ (long-dashed line).

For light-ion bombardment ($\mu>1$) the $\alpha$ function originally calculated by Sigmund severely overestimated the energy deposited at the surface because, in contrast to the situation in an experiment, the analytical theory allowed multiple scattering of projectiles through the reference plane ("surface") in the assumed infinite medium.[1,31] Bohdansky[9] suggested a crude correction term which equals the ratio of the projected to the total ion range. This correction seems to work reasonably well only in the range $1\leqslant\mu\leqslant10$. No theoretical basis exist for $\mu>10$. Previous work[9,26] suggests that $\alpha$ passes through a maximum at mass ratios $\mu$ between 5 and 20, similar to the fit through the data points of this study (long-dashed line in Fig. 9). There are several arguments to question the idea that $\alpha$ falls off sharply within a narrow range of $\mu$ values. First it is worth recalling that, according to analytical theory,[1] $\alpha$ depends on the mass ratio $\mu=M_2/M_1$. Hence $\alpha$ should be about the same for O, N, and C impact on Au ($12.3\leqslant\mu\leqslant16.4$) as for D on Si ($\mu=14$). According to Fig. 9, however, there is a difference by at least 50% between the Au and the Si data. One could suspect that this difference is related to the fact that the Au target was polycrystalline whereas the sputtered Si sample was amorphous. Such an argument, however, would exclude all sputtering yield data for polycrystalline metals from an analysis in terms of $\alpha$.

Much more likely is the idea that the sputtering yields for D on Si were reduced by bombardment induced incorporation of oxygen, as observed previously.[25] In fact, owing to the low sputtering yield of only 0.02 atoms/ion or less (Fig. 1), it is difficult to keep the bombarded surface dynamically clean. By contrast, the sputtering yield of polycrystalline Au and Au(111) bombarded with Ne exceeds 1 atom/ion at energies above 400 eV.[33] Moreover, Au does not react with oxygen. It is not difficult, therefore, to keep the surface of Au dynamically clean during sputtering with Ne or O. If we assume that the "true" $\mu$ dependence of $\alpha$ is represented by the thick solid line in Fig. 9, the measured sputtering yield for D on Si is lower than the true value by a factor of 1.32. For H on Si the corresponding factor is 1.84. This number is not unreasonable considering the fact that maximum yield reduction factors of about 5 have been observed as a result of oxygen incorporation in Si.[21,22] Even the He data in Fig. 1 show that differences in sputtering yield may be observed under presumably different residual gas pressures.

As to the low $\alpha$ values for H and D impact on polycrystalline Au, surface contamination is also likely to have played a role, not in the form of oxidation but probably more in the form of a carbonaceous surface layer. This supposition is supported by the fact that (i) the yields were also quite small (0.015 atoms/ion for H on Au), (ii) differed by up to 40% in repeated measurements at room temperature, and (iii) showed a clear trend for an increase in yield by up to a factor of 2 as the target temperature was raised (large effect already observed at 200–300 °C).[19] The latter observation suggests that surface cleaning occurred due to evaporation of adsorbed contaminants from heated targets (sputtering yield enhancement due to an evaporation related effect[34] can be excluded). Hence the sputtering yields for H and D on clean Au are also likely to be significantly larger than the mean values from which the $\alpha$ values in Fig. 9 were derived. After correction for surface contamination, the deviation from the suggested fit functions (solid lines) would disappear, partly or fully.

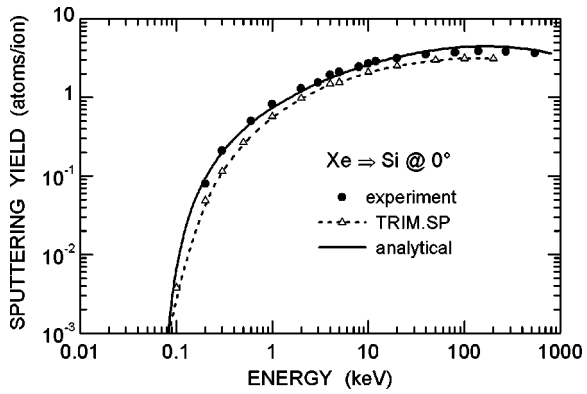


FIG. 10. Experimentally determined sputtering yields of Si for Xe bombardment at normal incidence (solid circles) compared with the predictions of the analytical yield formula (solid line). Also shown are results obtained by TRIM.SP computer simulations (Refs. 35 and 36).

### D. Absolute calibration of calculated sputtering yields

Up to now the experimental sputtering yields were discussed only in relative terms. To predict sputtering yields in absolute terms one needs to know two characteristic sample parameters, the areal density $x_0N$ of atoms contained within the mean escape depth $x_0$ and the surface binding energy $E_s$. The two unknown parameters determine the factor $k_n$ in Eq. (6). It is important to note that fitting of calculated to measured yields does not provide separate information about $x_0N$ and $E_s$, but only about the ratio $x_0N/E_s$. In Figs. 10–13 experimental data are compared with the predictions of analytical theory by setting $\tilde{x}_0N/\tilde{E}_s = 5\times10^{14}$ atoms cm$^{-2}$ eV$^{-1}$, where $\tilde{x}_0N$ and $\tilde{E}_s$ denote "effective" values of the respective parameters (see below). The other parameters entering into the analytical model were taken from Figs. 8 and 9. The agreement between theory and experiment is excellent for Xe, Ar, Ne, and He. There is some uncertainty at the low-energy end of the data where yield measurements are difficult, not only because of the danger of surface contamination but also because an accurate measurement of the ion energy is not a simple task. To illustrate the effect of a slight change in threshold energy, Figs. 11 and 12 also show yields calculated with $E_{\rm th}$ according to the fit function in Fig. 8.

As already discussed with reference to Fig. 9, the calculated yields for H and D are not as accurate as for the heavy primary ions. The measured yields and the derived $\alpha$ values appear to be lowered by oxygen incorporation. In Figs. 12 and 13 the yields calculated for (partially) oxidized and clean surfaces are labeled $\alpha_{\rm ox}$ and $\alpha_{\rm clean}$, respectively.

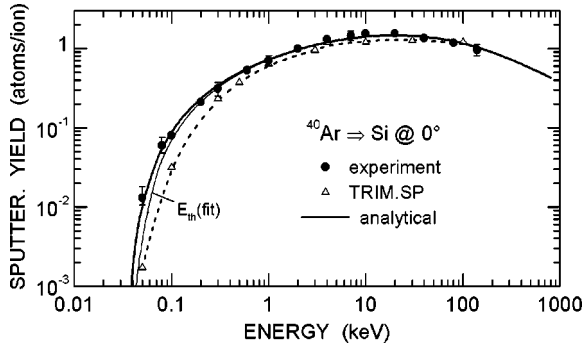


FIG. 11. The same as Fig. 10, but for Ar impact.

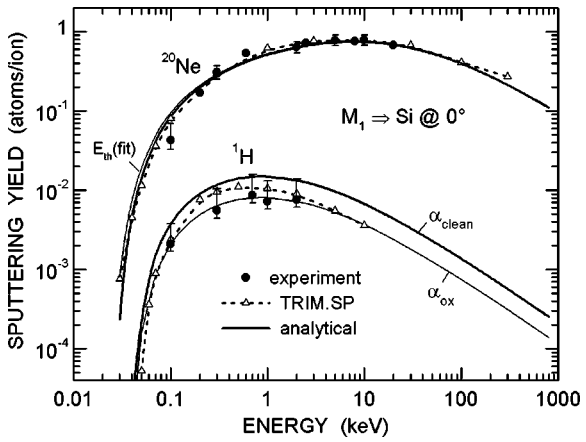


FIG. 12. The same as Fig. 10, but for H and Ne impact. The curves labeled $\alpha_{\rm clean}$ and $\alpha_{\rm ox}$ represent, respectively, empirical yields for Si with clean and partially oxidized surfaces.

Also shown in Figs. 10–13 are sputtering yields calculated by Eckstein[35,36] using the Monte Carlo code TRIM.SP.[30] The agreement between experiment and TRIM data is generally quite good although the simulations underestimate the yields for heavy-ion impact. It cannot be excluded, however, that the experimental Xe data are somewhat enhanced due to implanted and outdiffusing Xe atoms.[11,37] The threshold behavior predicted by the simulations differs slightly from the experimental data. The lower yields derived by TRIM for Ar and Xe could imply that the surface binding energy used in the simulations ($E_s = 4.7$ eV) was too high, an idea that is supported by the results of Fig. 8. If $E_s$ were reduced to 3.7 eV, the simulated data can be estimated to increase by 12%–14% (see Sec. III F). Hence we would get almost perfect agreement between TRIM, the experimental data, and the analytical fit for Xe and Ar, and still good agreement for Ne and He. The TRIM data for D and H would come very close to the yields predicted for clean Si surfaces. This reasoning supports the supposition that the experimental yields for H and D impact on Si were lowered by oxygen incorporation.

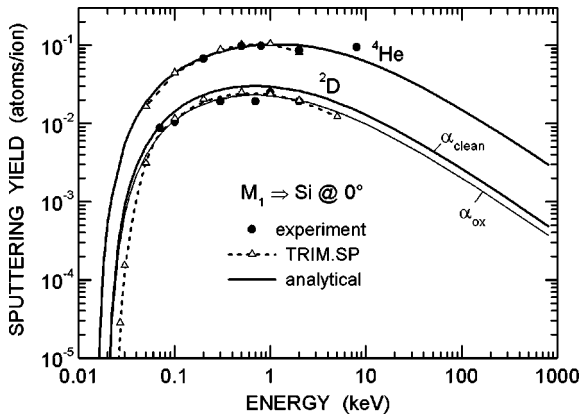


FIG. 13. The same as Fig. 12, but for D and He impact.

### E. Effective escape depth and effective surface binding energy

The last step in the data evaluation is an attempt to separate $\tilde{x}_0N/\tilde{E}_s$ into $\tilde{x}_0N$ and $\tilde{E}_s$. For this purpose one can make use of the light-ion results in Fig. 8 according to which $E_s = 3.7$ eV. This number may be considered the ''true'' surface binding energy in that it was derived from an idealized situation involving projectile-target interaction only in the first and second layers of the sample. Setting $\tilde{E}_s = E_s$ we have $\tilde{x}_0N = (\tilde{x}_0N/\tilde{E}_s)\ E_s = 1.85\times10^{15}$ atoms/cm$^2$, almost a factor of 2 larger than the value of $x_0N$ measured[6] and calculated[7,8] for keV ion bombardment. For $\tilde{x}_0N$ to become equal to $x_0N$ one would have to use an unreasonably low value for $E_s$—i.e., $(2\pm0.4\ \text{eV})$ eV. The problem can be solved by realizing that $x_0$ is defined on the basis of a depth convention according to which the outermost atom of a sample is located at depth $x=0$. Hence, if only the outermost atoms were sputtered, we would have $x_0=0$. Applying Eqs. (5) and (6) rigorously we would get $Y=0$, clearly an unrealistic result. Obviously $\tilde{x}_0N$ must be interpreted as the areal density of all atoms available for sputtering within the escape depth $x_0$, including the first layer with a mean areal density $N^{2/3}$. Accordingly,

$$\tilde{x}_0N = x_0N + N^{2/3}, \tag{15}$$

For Si, $N^{2/3} = 1.36\times10^{15}$ atoms/cm$^2$ so that $\tilde{x}_0N = 2.36\times10^{15}$ atoms/cm$^2$. Using this number to derive the effective surface binding energy we find $\tilde{E}_s = 4.7$ eV. Somewhat accidentally this is the ''standard'' value of the surface binding energy used in different simulations of Si sputtering.[7,8]

The evaluation outlined above implies that sputtering yields can be described on the basis of Eqs. (5) and (6) using a single calibration factor $\tilde{x}_0N/\tilde{E}_s$ for essentially all energies and mass ratios. This result is remarkable because, according to computer simulations,[7,8] $x_0$ increases with increasing bombardment energy. For Ar on Si, for example, $x_0$ values of 0.13 and 0.44 nm were calculated at 100 eV and 100 keV, respectively, an increase by more than a factor of 3 (Ref. 8). If these numbers were considered directly applicable in the present context, $\tilde{x}_0N$ should increase, according to Eq. (15), from 2.0 to $3.6\times10^{15}$ atoms/cm$^2$. With $\tilde{E}_s = \text{const}$, this implies an increase in $\tilde{x}_0N/\tilde{E}_s$ by a factor of 1.8 between 100 eV and 100 keV. However, the comparison of experimental and empirical yields in Fig. 8 does not provide any evidence for an energy dependent change in $\tilde{x}_0N/\tilde{E}_s$. A similar inconsistency is evident from the work of Glazov *et al.*[7] who calculated $Y$ and $x_0$ for 1 and 3 keV Ne on Si at almost normal incidence (2° off). According to Eqs. (5) and (6) we should have $Y_{3k}/Y_{1k} = (x_0s_n)_{3k}/(x_0s_n)_{1k}$. However, the ratios derived from the calculated data are $Y_{3k}/Y_{1k} = 1.34$, $(x_0\ s_n)_{3k}/(x_0\ s_n)_{1k} = 1.80$, and $(\tilde{x}_0s_n)_{3k}/(\tilde{x}_0s_n)_{1k} = 1.47$; i.e., a significant difference between the analytical formalism and computer simulations is evident even for a change in energy by only a factor of 3.

In this context it is worth noting that the distributions of the depth of origin, calculated for different bombardment energies, feature a similar shape at depths between 0 and 0.25 nm, but differ significantly in the long-range tail which extends to larger depths the higher the energy.[8] On the other hand, the depth of origin contained in Eq. (1) was defined under the assumption[1] that the energy loss of sputtered particles between their point of origin and the surface can be neglected. Including energy loss, slightly larger values of $x_0$ were expected.[1] This supposition was verified by analytical estimates.[38]

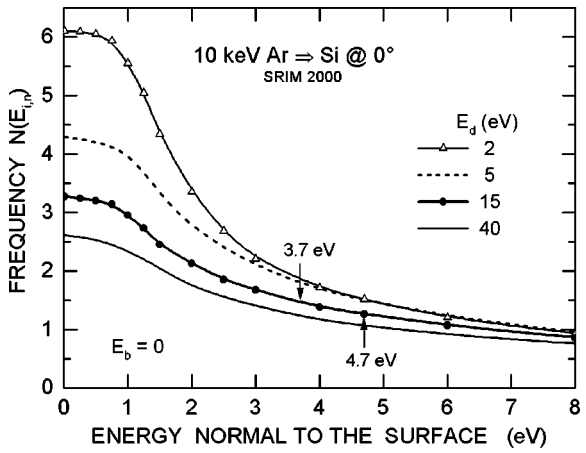


FIG. 14. Calculated frequency distribution of the mean number of target atoms arriving at the inner surface of an Ar bombarded Si sample. Simulations performed for different displacement energies $E_d$.

### F. Effect of the displacement energy and lattice binding energy

The significant (>20%) difference between $E_s$ and $\tilde{E}_s$ brings up the old question whether the surface binding energy is the only binding force determining the sputtering yield. Sigmund has repeatedly discussed conceivable effects of the interatomic bond strength or bulk (lattice) binding energy $E_b$ and the displacement threshold energy $E_d$. He concluded,[31] ''...it appears appropriate to assume that $E_d$ is immaterial in the evaluation of the sputtering yield.'' The bulk binding energy $E_b$, on the other hand, was considered important.[1,31] He presented some estimates of $Y(E_b)$ (see below), but finally decided to stay with Eq. (1), solving ''the problem (of interpreting $E_s$) by definition.'' [1] The influence of $E_b$ and $E_d$ on $Y$ has not been discussed seriously since then. A significant effect of $E_d$ on $Y$ was identified some time ago by computer simulations of Roush *et al.*[39] Analysis of the data showed that the calculated yields depend nonlinearly on $E_d$ (Ref. 37).

In this study the effect of $E_d$ and $E_b$ on the sputtering yield was explored using the SRIM 2000 simulation code.[40] The code allows simulations to be performed with $E_s$, $E_b$, and $E_d$ as freely selectable input parameters. A recent evaluation has shown that SRIM 2000 does not predict the mass dependence of sputtering yields correctly at mass ratios $M_1/M_2 < 1$ (Ref. 41). Here, sputtering yields were calculated for 10 keV Ar bombardment of Si, in which case the code appears to work reasonably well. One type of information provided by the code is the integral number of target

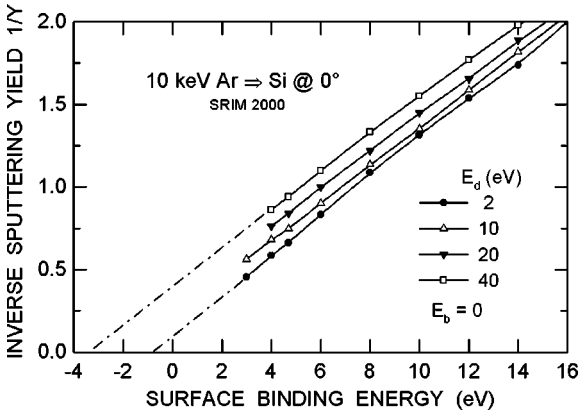


FIG. 15. Calculated inverse sputtering yield vs the surface binding energy, for different values of the displacement energy. The dash-dotted lines are linear extrapolations to the limit $1/Y \rightarrow 0$.

atoms $N(E_{i,n})$, arriving at the surface with an (internal) energy $E_{i,n}$ normal to the surface. The sputtering yield is simply $Y = N(E_{i,n} > E_s)$. Examples of the dependence of $N(E_{i,n})$ on $E_d$ are presented in Fig. 14. In qualitative agreement with the early work of Roush *et al.*,[39] the sputtering yield $N(E_s)$ decreases with increasing $E_d$. The effect of $E_d$ on $Y$ is larger the lower the surface binding energy.

According to Eq. (1) the inverse sputtering yield should be proportional to the surface binding energy, $Y^{-1} \propto E_s$. As Fig. 15 shows, the simulated results are in good agreement with the predicted linear behavior. Deviations from linearity are observed at energies $E_{i,n} < 3$ eV (data not shown in Fig. 15). The slope of the straight lines is $d(1/Y)/dE_s = 12\%/\text{eV}$. It is worth noting that the dash-dotted lines in Fig. 15, obtained by linear extrapolation of the different curves to the limit $Y^{-1} \rightarrow 0$ (i.e., $Y \rightarrow \infty$), do not cross the abscissa at $E_s = 0$, as Eq. (1) predicts, but intersect at larger values of $E_s$ the larger $E_d$.

Figure 16 shows the dependence of calculated sputtering yields on $E_d$, with $E_s$ as a parameter. As already noted with reference to Fig. 14, the effect of $E_d$ on the sputtering yield is larger the smaller $E_s$. For hypothetical surface binding energies $E_s > 10$ eV, however, the $E_d$ effect on the yield disappears completely. Even for small surface binding energies, the $E_d$-dependent yield changes become rather small as $E_d$ exceeds 30 eV. This is the region $E_d \geqslant 10E_s$ specifically considered by Sigmund, arriving at the conclusion that the displacement energy is immaterial in sputtering.[31]

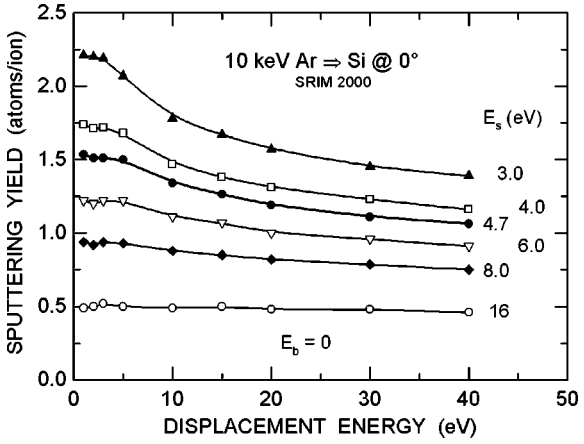


FIG. 16. Calculated sputtering yields vs the displacement energy, for different values of the surface binding energy.

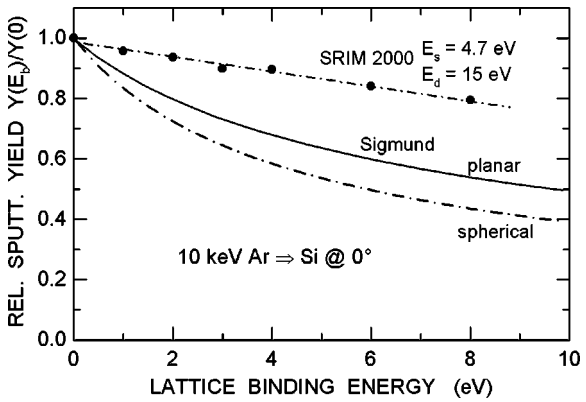


FIG. 17. Calculated sputtering yields vs the lattice binding energy, normalized to the yield for $E_b = 0$ (solid circles and dash-dotted line). Estimates by Sigmund (Ref. 1) are shown for comparison.

The $E_b$ effect on the sputtering yield was also investigated by SRIM 2000, using $E_s = 4.7$ eV and $E_d = 15$ eV as fixed input parameters. The results are presented in Fig. 17 in the form of relative sputtering yields, normalized to the yield for $E_b = 0$. The SRIM data (solid circles) suggest that the sputtering yield decreases linearly with increasing lattice binding energy, but the slope of the linear fit through the data points is quite small, $(1/Y(E_b = 0))dY/dE_b \cong 2.5\%/\text{eV}$. In view of the uncertainties with respect to $E_s$ and $E_d$, it is hard to see a justification for performing simulations with bulk binding energies other than $E_b = 0$. De Witte *et al.*[42] have obtained the ''best results'' of computer calculations using $E_s = 2.72$ eV(!), $E_b = 2$ eV, $E_d = 15$ eV, in combination with a modified electronic stopping power. Considering the results of Figs. 15–17 this rather unusual combination of binding energies cannot be considered unique (note, in particular, the unrealistically low value of $E_s$).

Also shown in Fig. 17 are the predictions of Sigmund[1] for planar and spherically symmetric surface potential barriers (a planar potential was commonly assumed in recent computer simulations). The predicted decrease in yield with increasing lattice binding energy is significantly larger than the effect calculated by SRIM.

The relevance of the results in Figs. 14–16 rests on the assumption that the SRIM 2000 simulation code is reliable. As pointed out above, the mass dependence of sputtering yields calculated with SRIM was found to be in error for $M_1/M_2 < 1$. On the other hand, an effect of $E_d$ on the sputtering yield was also found using the code EVOLVE.[39] However, if Sigmund's arguments are considered a convincing guide line, we have to conclude that SRIM as well as EVOLVE does not predict sputtering phenomena correctly. Clearly, this is yet another example of the well-known problem that many authors of simulation codes do not provide sufficient evidence that the program will always yield results in accordance with the underlying physics.

To retain the simple concept of the analytical theory expressed in Eq. (1), we have to look for physically meaningful processes which have the effect of keeping $\tilde{x}_0 N/\tilde{E}_s$ constant even though, according to presumably reliable computer simulations,[7,8] the mean escape depth $\tilde{x}_0 N$ increases with increasing impact energy. To compensate this increase we either need an equivalent increase of the parameter $\tilde{E}_s$ or an additional factor in the numerator which decreases with increasing energy. One idea not discussed up to now is that the energy $S_n$ deposited into nuclear motion at the surface is partly consumed in inelastic processes and the creation of phonons and damage (displaced atoms). The net effect would be the same as an increase in the effective surface binding energy.

## IV. SUMMARY AND CONCLUSION

This study has shown that it is possible to describe the sputtering yields of silicon for normally incident ions in analytical form, from the regime of single knock-on events to fully developed collision cascades. The energy dependence of the sputtering yield can be accounted for by the reduced nuclear stopping cross section and the threshold function. The $\alpha$ function and the threshold energies contained in the $\eta$ function apparently depend only on the mass ratio $\mu$. Any additional energy or mass dependent function is not required. Using the analytical model, most of the experimentally determined sputtering yields could be reproduced with an accuracy of about $\pm 15\%$ or better. Some problems still exist with the respect to very low yields ($<0.05$) observed under impact of either very light primary ions (H and D) or heavy ions at very low energies ($\leqslant 200$ eV). Presumably due to surface contamination, the reported yields appear to be lower than the true values that one would measure if the sample surfaces were clean during sputter erosion.

Yield measurements with light ions ($\mu > 5$) at energies up to about 10 times the threshold energy appear to be well suited for determining the true surface binding $E_s$ which turned out to be distinctly lower than the effective surface binding energy $\tilde{E}_s$ contained in the yield calibration factor $\tilde{x}_0 N/\tilde{E}_s$. This calibration factor was found to be constant within experimental accuracy. The origin of the apparent difference between $E_s$ and $\tilde{E}_s$ needs to be studied in more detail. Reasonable values for $\tilde{E}_s$ can only be obtained if $\tilde{x}_0 N$ is set equal to the areal density of all atoms contained within the mean escape depth of sputtered atoms.

Another important conclusion is that sputtering yield data are not suited for deriving detailed information on nuclear stopping cross sections. The first reason is that, at reduced energies $\varepsilon > 10^{-2}$, the difference in the energy dependence of the different versions of $s_n$ is smaller than the uncertainty of experimentally determined sputtering yields. Differences in the maxima of the proposed $s_n$ functions contribute a relative uncertainty of about $\pm 10\%$ to the calibration factor $\tilde{x}_0 N/\tilde{E}_s$. The second reason is that, even for heavy-ion bombardment, the sputtering yields at low energies ($\varepsilon < 10^{-2}$) are dominated by threshold effects, more so the lower the energy. The sometimes significant differences between cross sections at low $\varepsilon$ cannot be used for $s_n$ selection because these differences can easily be accounted for by a slight adjustment of the threshold energy which, unfortunately, is not a known input parameter.

As to future research, more detailed studies are clearly desirable, experimentally as well as by computer simulation. The data basis presently available at low energies is not yet satisfactory, notably for light ions. Recent advances in ion-gun technology,[43] driven by the need for sputter depth profiling near the physical limits of depth resolution,[44] now allow sputtering experiments in ultrahigh vacuum to be performed routinely at beam energies down to 150 eV. Hence surface contamination should no longer be a problem of concern. Furthermore, using $\delta$-doped samples, one could determine sputtering yields at much smaller primary ion fluences than with the mass loss technique. This approach would also allow an identification of conceivable fluence dependent sputtering artifacts.[45]

The computer calculations performed in course of this study should be viewed with reservation because the SRIM 2000 code suffers from ill-defined inaccuracies. Other more reliable computer codes should be used to determine the dependence of sputtering yields on the various input parameters. Such calculations, carried out for light- and heavy-ion bombardment, should be of help in trying to distinguish the ''true'' surface barrier $E_s$ for sputter ejection, as defined by Eq. (9), from the ''apparent'' surface binding energy $\tilde{E}_s$ which implicitly contains contributions due to all binding forces.

## ACKNOWLEDGEMENT

I thank W. Eckstein for helpful discussions.

[1] P. Sigmund, Phys. Rev. **184**, 383 (1969).
[2] N. Bohr, Mat. Fys. Medd. K. Dan. Vidensk. Selsk. **18**, no. 8 (1948).
[3] J. F. Ziegler, J. P. Biersack, and U. Littmark, *The Stopping and Range of Ions in Solids* (Pergamon, New York, 1985).
[4] J. Lindhard, M. Scharff, and H. E. Schiøtt, Mat. Fys. Medd. K. Dan. Vidensk. Selsk. **33**, no. 14 (1963).
[5] M. Vicanek, J. J. Jiminez Rodriguez, and P. Sigmund, Nucl. Instrum. Methods Phys. Res. B **36**, 124 (1989).
[6] K. Wittmaack, Phys. Rev. B **56**, R5701 (1997).
[7] L. G. Glazov, V. I. Shulga, and P. Sigmund, Surf. Interface Anal. **26**, 512 (1998).
[8] V. I. Shulga and W. Eckstein, Nucl. Instrum. Methods Phys. Res. B **145**, 492 (1998).
[9] J. Bohdansky, Nucl. Instrum. Methods Phys. Res. B **2**, 587 (1984).

[10] J. Bohdansky, J. Roth, and H. L. Bay, J. Appl. Phys. **51**, 2861 (1980).
[11] P. Blank and K. Wittmaack, J. Appl. Phys. **50**, 1519 (1979).
[12] H. E. Roosendaal, in *Sputtering by Particle Bombardment I*, edited by R. Behrisch (Springer, Berlin, 1981), Chap. 5.
[13] P. C. Zalm, J. Appl. Phys. **54**, 2660 (1983).
[14] K. Wittmaack and D. B. Poker, Nucl. Instrum. Methods Phys. Res. B **47**, 224 (1990).
[15] D. J. Oostra, R. P. van Ingen, A. Haring, A. E. de Vries, and G. N. A. van Veen, Appl. Phys. Lett. **50**, 1506 (1987).
[16] N. Laegreid and G. K. Wehner, J. Appl. Phys. **32**, 365 (1961).
[17] D. Rosenberg and G. K. Wehner, J. Appl. Phys. **33**, 1842 (1962).
[18] J. Roth, J. Bohdansky, and A. P. Martinelli, Radiat. Eff. **48**, 213 (1980).
[19] W. Eckstein, C. García-Rosales, J. Roth, and W. Ottenberger, *Sputtering Data* (Max-Planck-Institut für Plasmaphysik, Garching, 1993).
[20] E. H. Hasseltine, F. C. Hurlbut, N. T. Olson, and H. P. Smith, Jr., J. Appl. Phys. **38**, 4313 (1967).
[21] A. E. Morgan, H. A. M. de Grefte, N. Warmoltz, H. E. Werner, and H. J. Tolle, Appl. Surf. Sci. **7**, 372 (1981).
[22] W. Wach and K. Wittmaack, J. Appl. Phys. **52**, 3341 (1981).
[23] K. Wittmaack and S. F. Corcoran, J. Vac. Sci. Technol. B **16**, 272 (1998).
[24] M. Saidoh, H. L. Bay, J. Bohdansky, and J. Roth, Nucl. Instrum. Methods Phys. Res. B **13**, 403 (1986).
[25] K. Wittmaack and G. Staudenmaier, J. Nucl. Mater. **93&94**, 581 (1980).
[26] C. García-Rosales, W. Eckstein, and J. Roth, J. Nucl. Mater. **218**, 8 (1994).
[27] W. D. Wilson, L. G. Haggmark, and J. P. Biersack, Phys. Rev. B **15**, 2458 (1977).
[28] N. Matsunami, Y. Yamamura, Y. Itikawa, N. Itoh, Y. Kazamata, S. Miyagawa, K. Morita, and R. Simizu, Radiat. Eff. Lett. **50**, 39 (1980).
[29] H. H. Andersen, Mat. Fys. Medd. K. Dan. Vidensk. Selsk. **43**, 127 (1993).
[30] J. P. Biersack and W. Eckstein, Appl. Phys. A: Solids Surf. **34**, 73 (1984).
[31] P. Sigmund, in *Sputtering by Particle Bombardment I*, edited by R. Behrisch (Springer, Berlin, 1981), Chap. 2.
[32] H. H. Andersen and H. L. Bay, J. Appl. Phys. **45**, 953 (1974); **46**, 2416 (1975).
[33] W. Szymczak and K. Wittmaack, Nucl. Instrum. Methods Phys. Res. B **82**, 220 (1993).
[34] K. Besocke, S. Berger, W. O. Hofer, and U. Littmark, Radiat. Eff. **66**, 35 (1982).
[35] W. Eckstein, Surf. Interface Anal. **14**, 799 (1989).
[36] W. Eckstein, *Calculated Sputtering, Reflection and Range Values* (Max-Planck-Institut für Plasmaphysik, Garching, 2002).
[37] K. Wittmaack, Nucl. Instrum. Methods Phys. Res. B **2**, 569 (1984).
[38] G. Falcone and P. Sigmund, Appl. Phys. **25**, 307 (1981).
[39] M. L. Roush, T. D. Andreadis, F. Davarya, and O. F. Goktepe, Nucl. Instrum. Methods Phys. Res. **191**, 135 (1981).
[40] J. F. Ziegler and J. P. Biersack, http://www.SRIM.org/
[41] K. Wittmaack (unpublished).
[42] H. De Witte, W. Vandervorst, and R. Gijbels, J. Appl. Phys. **89**, 3001 (2001).
[43] N. S. Smith, M. G. Dowsett, B. McGregor, and P. Phillips, in *Secondary Ion Mass Spectrometry SIMS X*, edited by A. Benninghoven, B. Hagenhoff, and H. G. Werner (Wiley, Chichester, 1997), p. 363.
[44] K. Wittmaack, Surf. Interface Anal. **21**, 323 (1994).
[45] K. Wittmaack, J. Vac. Sci. Technol. B **18**, 1 (2000).